Hindawi
Mathematical Problems in Engineering
Volume 2019, Article ID 7036538, 12 pages
https://doi.org/10.1155/2019/7036538

Research Article

Road Tunnel Axial Fan Performance In Situ Test: Taking Qinling Zhongnan Mountain Highway Tunnel as an Example

Yongdong Wang, Xingbo Han, Tianyue Zhou, Zhiwei He, Feilong Tian, Zhuoqi Zheng, and Haiping Zhao

School of Highway Engineering, Chang'an University, Xi'an 710064, Shaanxi, China

Correspondence should be addressed to Yongdong Wang; wydchdgl@163.com and Xingbo Han; xingbo.han@chd.edu.cn

Received 9 November 2018; Revised 8 March 2019; Accepted 21 March 2019; Published 4 April 2019

Academic Editor: Andras Szekrenyes

Axial fans play a pivotal role in the road tunnel ventilation system. Qualified performance of the axial fan is important for both safety and air quality maintenance reasons. Axial fans performance in situ test of Qinling Zhongnan Mountain highway tunnel, the second longest road tunnel in the world, is presented in this research. Performance test items and the qualification criterion, as well as a general framework for the road tunnel axial fan assessment, are recommended. Log-Tchebycheff method is suggested to confirm the location for the measuring lines and points. The precision of the log-Tchebycheff method in air flow rate measuring is verified by comparing with the biharmonic spline interpolation fitting result. The research shows that the log-Tchebycheff method has high precision and good efficiency in the air flow rate measurement of the road tunnel air duct. What is more, the biharmonic spline interpolation fitting method can be applied to obtain a more accurate result. The number of interpolation points of the biharmonic spline interpolation fitting method should be bigger than 2000 to provide quality results.

1. Introduction

Ventilation plays a critical role in both normal operating [1] and fire [2, 3] situations of a tunnel. It should keep the air pollutant such as CO_X, NO_X, and smoke dust in low concentration, prevent the smoke back layering, and exhaust smoke [4–6] out of the tunnel. Especially, long tunnels necessitate a fine-tuned control of the ventilation system for safety and air quality maintenance reasons [7, 8]. Axial fans and jet fans constitute the main part of the tunnel ventilation system. Indoor or numerical researches on jet fans preference are extensively established [9–15]. For axial fans, it is generally diagnosed by comparing the fan performance curve provided by the fan manufacturer with the required performance parameters of the designed tunnel. Usually, the fan performance curve provided by the manufacturer is obtained from their laboratory test. However, there exists a great difference between the laboratory performance curve and the in situ one for reasons such as the fan misalignment, operating environment diversity, and added structures (including diffusion tube, collector, muffler, etc.). On the other hand, the ageing of the axial fan could also bring a reduction to its performance. The average efficiency of fans is only 57% [16] at present and most of them service far different from their designed working point. Thus, an in situ test is urgently needed to determine whether the axial fan is still sufficient at the designed point when to be installed in the real tunnel fan room environment as well as with time ageing.

To date, the axial fan in situ test has gained much attention in the mine ventilation [17–21], but little attention has been given to the road tunnels. It takes granted that research fruits such as mine fan static pressure and motor parameters tests can be used for reference in the tunnel axial fan in situ test. However, first and foremost, air flow rate measurement during the performance test of the tunnel fans is much more difficult than mine fans. The cross-section area of the tunnel air duct is usually two to three times than that of the mine air duct and is always much shorter. For these reasons, the wind field of road tunnel air duct is more disordered which brings difficulty to the precision measurement of the air flow rate.

The air flow rate in a section of tunnel or air duct may be determined in two ways: either by measuring the pressure difference produced by a differential pressure device (orifice plate, venturi tube, nozzle, or pitot tube) or by

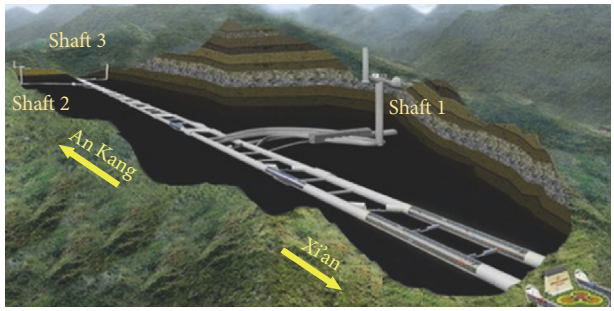

Figure 1: Three-shaft ventilation of Qinling Zhongnan Mountain highway tunnel.

determining the velocity at various points in this section and then calculating the mean velocity. The pressure difference method is divided into dynamic and static methods. Two cross sections with different areas and static air flows, which are always difficult to select, are required in the static pressure difference method. Similarly, the dynamic difference method requires a large number of pitot tubes, which always produces an air leak problem. In addition, a conversion between the test result and air velocity is needed before we can obtain the air flow rate with these two methods. In contrast, the air velocity method can provide the air flow rate directly and is extensively applied in fan performance in situ tests.

Air velocity method has been used and developed by researches in different fields. Single point measurement is the most common method used in air flow rate tests [22]. Only a single point of air velocity was tested and treated as the average velocity of each test section among these studies. Considering the inaccuracy of single point measurements, Qiu et al. [23] divided the test section into several parts in their study on the friction coefficient of a shot concrete lining. The air velocity at the centroid of each small part was measured, and their arithmetic mean was regarded as the mean air velocity of the section. Similar method was performed by Wang et al. [24, 25], Fang et al. [26], and Ren et al. [27] during the ventilation performance testing of a complementary ventilation tunnel. Compared with the single point measurement, these multipoint experiments were more accurate. However, the data for every point were not measured at the same time [28]. To obtain all of the multipoint measurement data simultaneously, Yang et al. [29] investigated a tunnel's ventilation performance via several wind cups. A tunnel section was also divided into equal area parts, and a steel frame for supporting the wind cup was used in this experiment. All the air velocities could be measured at the same time. A five-point truss was utilised by Levoni et al. [28] to investigate the fluid dynamic characterisation of the Mont Blanc tunnel. These simultaneous multipoint velocity measurements constitute the available method for collecting reliable mean air velocity data along a tunnel's cross section and estimating the total flow rate.

This is because the influence of the tunnel walls and disordered distribution of the air velocity along its cross section make direct measurements of the air flow rate a very difficult task. Usually, the flow velocity is zero at the tunnel lining wall and reaches its maximum at the centre of the cross section. The velocity distribution between the tunnel wall and cross-section centre changes with the flow condition of the air [30]. The weights of the measuring points in the above methods are all equal. Therefore, the velocity change along the tunnel section is ignored in these methods. Thus, a simultaneous multipoint air flow measurement method that considers the air distribution of the tunnel cross section is urgently needed.

To have road tunnel axial fans assessed, this work firstly presents the performance test items and qualification criterion for road tunnel axial fans. Then, combined with the in situ test of Qinling Zhongnan Mountain highway tunnel, the general process of an axial fan assessment is stimulated. What is more, thought a theoretical analysis, the log-Tchebycheff method is suggested to confirm locations for measuring lines and points. Its precision in air flow rate measuring is verified by comparing with the MATLAB fitting results. Finally, the performance of the axial fan of the tunnel is assessed via performance curves established by the in situ result.

2. Engineering Background

The Qinling Zhongnan Mountain highway tunnel is 18020 m long, making it the longest tunnel in Asia and the second longest road tunnel in the world. A three-shaft ventilation system is used for the Qinling Zhongnan Mountain highway tunnel (Figure 1). A total of 32 high-power axial fans were installed in the three ventilation shafts. Shaft 1 has nine fans: four exhaust fans and five inlet fans. Shaft 2 has 12 fans: six exhaust fans and six inlet fans. Shaft 3 has 11 fans: five exhaust fans and six inlet fans. The inlet fans were made by the South Fan Company of China. The exhaust fans were made by the Flack Woods Company in the UK.

The detailed structure of the shaft 1 is shown in Figure 2. The axial fans are located in an excavated underground fan room (red circles in Figure 2). Denote that the drive direction of the left line of the main tunnel is from An Kang to Xi'an. The drive direction of the right line is from Xi'an to An Kang. As can be seen from Figure 2, the direction of the air flow of both left and right lines is the same as the drive direction. In this way, the pressure caused by the traffic flow can be used as an impetus rather than a resistance of the tunnel ventilation. The air flow direction is quite clear by applying the three shafts in this tunnel. The polluted air will be firstly discharged by the exhaust fans via the air output duct. Then, the fresh air

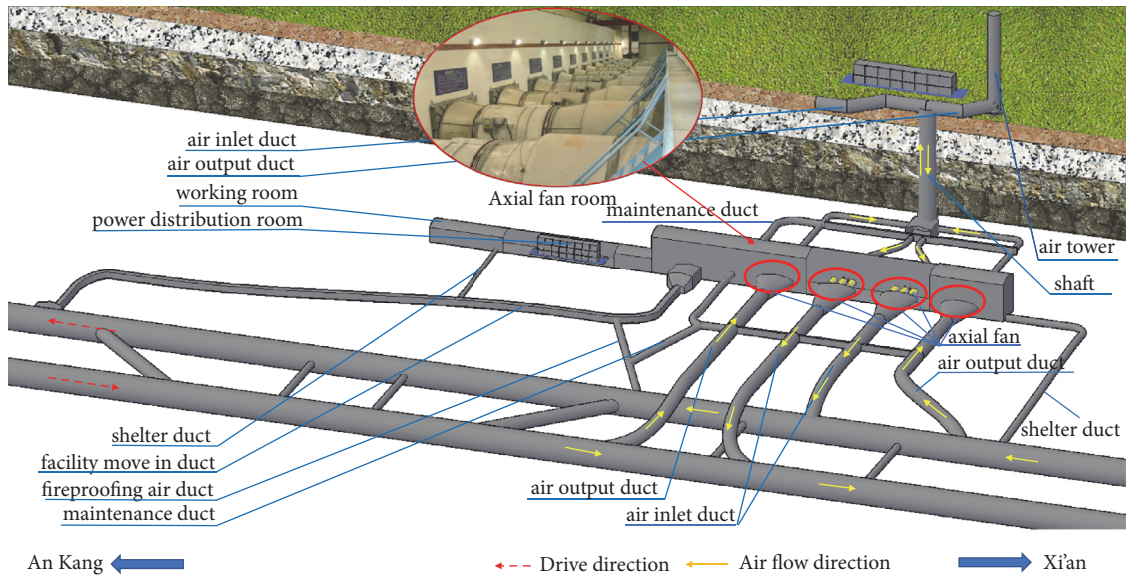

Figure 2: Detailed structure and ventilation control of shaft 1.

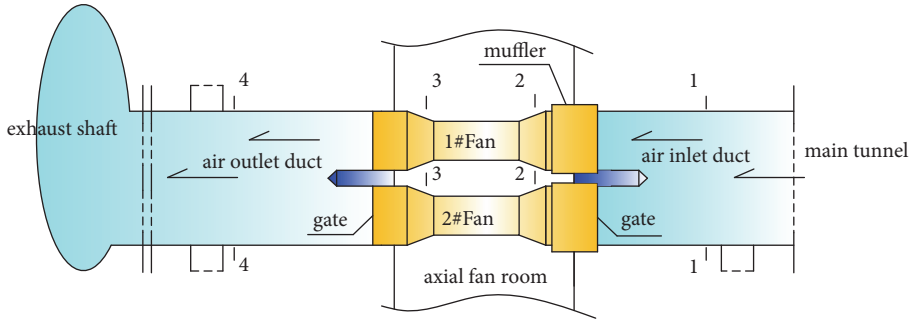

Figure 3: Ventilation network of the tunnel axial fan.

will be brought into next section of the main tunnel by inlet fans via the air inlet duct (yellow arrows in Figure 2).

3. Assessment Criteria and Test Items

3.1. Assessment Criteria. For road tunnels, four items are recommended here to verify an eligible axial fan:

3.1.1. Maximum Air Flow Volume. Tunnel ventilation axial fans must provide sufficient volume of fresh air to keep the tunnel operating environment qualified in its CO concentration and visibility. Thus, the maximum volume of an axial air flow rate should be greater than the required fresh air volume.

3.1.2. Difference between the Tested Total Pressure and Designed Total Pressure at the Designed Operating Point. To ensure the newly installed or service fans work as it designed and keep its performance, the difference between the tested total pressure and designed total pressure should be limited within 5%.

3.1.3. Fan Motor Capacity Safety Factor. The fan motor must have sufficient motivation to maintain the fan's operation, pony cart is not allowed here. The highway tunnel design code of China [31] has stipulated that the fan motor capacity safety factor should be bigger than 1.1.

3.1.4. Total Pressure Efficiency at the Designed Operating Point. The daily electricity consumption of the operation of Qinling Zhongnan Mountain highway tunnel is 12652 kW·h (equivalent to 1890 US dollars). The ventilation costs account for more than 70% [31] of the total electricity consumption. Thus, the high efficiency of the axial fan is significant to the energy-saving operation of tunnels. The recommended lower limit of fan total pressure efficiency is 70%[31].

3.2. In Situ Items and Methods. The fan performance curves consist of volume, total pressure curve; volume, axial power curve; and volume, efficiency curve. Take Qinling Zhongnan Mountain highway tunnel as an example, to obtain the most reliable test data, the ventilation network during the in situ test was the same as that used during its daily operation. As shown in Figure 3, air from the main tunnel was firstly discharged into the air inlet duct and then travelled across the axial fan. Finally, it was blown into the shaft via the air outlet duct. The calculation process of the fan air flow rate, fan total

pressure, axial power, efficiency and fan motor capacity safety factor will be presented in detail in the flowing sections.

3.2.1. Fan Air Flow Rate. As shown in Figure 3, the air flow rate of the fan at the cross section 3-3 was difficult to be measured. Fortunately, the air flow rate at 4-4 was easy to be measured. The mass flow rate at each section of the duct is the same. Thus, the air flow rate measurement section was chosen as the cross section 4-4. Once the mass flow rate of the duct could be determined, the volume flow rate of the fan (section 3-3) could then be obtained.

The relationship between the mass flow rate and the volume flow rate can be presented as follows:

$$q_{\mathrm{m}} = \rho_4 q_{4\mathrm{v}} \tag{1}$$

where q_{m} is the mass flow rate, $q_{4\mathrm{v}}$ is the total volume flow rate of the cross section 4-4 which can be determined by the air flow rate measurement, ρ_4 is the air density of the cross section 4-4 which can be determined by using the following equation:

$$\rho_{\mathrm{i}} = \frac{0.00348\left(p_{\mathrm{is}} - 0.3779\varphi p_{\mathrm{sh}}\right)}{273.15 + t} \tag{2}$$

where ρ_{i} is the air density of the cross section *i-i* (kg/m^3), p_{is} is the absolute static pressure of the cross section *i-i* (Pa), φ is the relative humidity (%), t is the temperature (°C), and p_{sh} is the air absolute saturated steam pressure at temperature t in Pa.

The precise measurement of the total volume flow rate ($q_{4\mathrm{v}}$ for section 4-4) was the most difficult work in this in situ test. The velocity-area method has been proven to be one of the most accurate methods for the air flow rate measurement. However, the position of measurement points has great influence on the accuracy of test results. Previous research [32] showed that the log-Tchebycheff method could provide more accurate test results than the equal area method. Thus, the log-Tchebycheff method was recommended in this work. The air velocity in the tunnel is not homogeneous along its cross section. The air velocity distribution is disordered and difficult to regulate. Thus, it is necessary to divide the cross section into many parts. If each part is small enough, the velocity of this small part could be treated as a constant. Then, the total flow rate could be represented by the following equation:

$$q_{\mathrm{iv}} = \sum A_{\mathrm{i}} v_{\mathrm{i}} \tag{3}$$

where q_{iv} indicates the air flow rate of the tunnel cross section *i-i*, A_{i} is the area of the ith part, and v_{i} is the velocity of the ith part.

Considering the air in the tunnel to be a fully developed turbulent flow, the boundary condition at the tunnel surface can be expressed as follows:

$$\left.\frac{\partial v}{\partial y}\right|_{y=0} = 1, \quad v|_{y=0} = 0 \tag{4}$$

The boundary condition at the centre of the section is as follows:

$$\left.\frac{\partial v}{\partial y}\right|_{y=R} = 0, \quad v|_{y=R} = v_{\max} \tag{5}$$

where v is the axial velocity of a point of the tunnel cross section, y is the distance between the point and the tunnel wall surface, R is the hydraulic radius of the tunnel, and the dimension of velocity gradient $\partial v/\partial y$ is (s^{-1}).

The velocity model should be considered in two parts. The first part is the velocity distribution of the zone near the wall. The velocity distribution of this part is in line with the following properties:

$$v^+ = \frac{1}{K}\ln y^+ + B \quad \left(5 < y^+ < 7^B\right) \tag{6}$$

where v^+ is the dimensionless flow velocity, $v^+ = v/v*$, $v*$ indicates the shear stress velocity, $v* = \sqrt{\tau}/\rho$, τ is the shear stress, ρ is the air density, y^+ is the dimensionless distance to the tunnel surface, and K and B are constant.

The second part is the zone away from the tunnel wall. The velocity distribution of this part is in line with the following polynomial [33]:

$$v = a_0 + a_1\left(\frac{r}{R}\right)^2 + a_2\left(\frac{r}{R}\right)^4 + \cdots + a_N\left(\frac{r}{R}\right)^{2\mathrm{N}} \tag{7}$$

where $a_0, a_1, a_2, \ldots, a_{\mathrm{N}}$ are constant, N is the number of measuring points in the same radius, and r is the distance to the tunnel centre.

Taking into account the wind tunnel airflow distribution, the true function of the flow rate distribution on the two parts $f(\mathrm{x})$ could be approximately expressed by Tchebycheff polynomials $P(\mathrm{x})$, $f(x) \in \mathrm{C}[-1, 1]$. If we let $x = \cos\theta$, $\theta \in \mathrm{C}[0, \pi]$ and $g(\theta) = f(\cos\theta)$ can be expanded into the following cosine series:

$$g(\theta) = \frac{1}{2}a_0 + \sum_{N=1}^{\infty} a_{\mathrm{N}} \cos N\theta \tag{8}$$

The $(N+1)$th order Tchebycheff polynomial [34] is expressed as

$$T_{\mathrm{N+1}} = \cos(N+1)\theta \tag{9}$$

When $\cos\theta = x$, (9) can be reexpressed as follows:

$$T_{\mathrm{N+1}}(x) = \cos\left[(N+1)\arccos x\right] \tag{10}$$

Let $(N+1)\arccos x = (2k+1)\pi/2$ $(k = 0, 1, \ldots, N)$; the Tchebycheff nodes can be expressed as follows:

$$x_{\mathrm{k}} = \cos\frac{(2k+1)\pi}{2} \tag{11}$$

The nodes can be transferred from $x \in [-1, 1]$ to any common situation $x \in [a, b]$ by using the following equation:

$$x = \frac{1}{2}\left[(b-a)t - a + b\right] \tag{12}$$

Thus, the new interpolation nodes can be calculated as follows:

$$x_{\mathrm{k}} = \frac{b-a}{2}\cos\frac{(2k+1)\pi}{2(N+1)} + \frac{a+b}{2} \quad k = 0, 1, \cdots, N \tag{13}$$

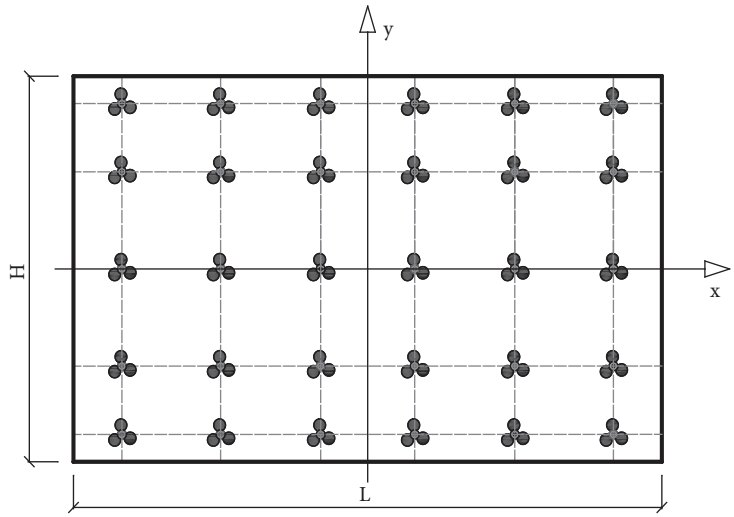

Figure 4: Rectangular section point distribution.

Table 1: Measuring point distribution.

e or f	x_i/L or y_i/H			
5	/	0	0.212	0.426
6	/	0.063	0.265	0.439
7	0	0.134	0.297	0.447

Table 2: Specific test line and point distribution according to Tchebycheff method.

Measuring lines or points	1	2	3	4	5	6
x_i/L	0.075	0.235	0.437	0.563	0.765	0.925
y_i/h_i	0.061	0.235	0.437	0.563	0.765	0.939

Locations of measure points in the rectangular section determined by the log-Tchebycheff method are shown in Figure 4, and the specific coordinates are listed in Table 1. The mean velocity can be calculated by the following considering an equal weight for each measuring point:

$$\overline{v} = \frac{\sum_{i=1}^{e,f} v_{\mathrm{im}}}{ef} \tag{14}$$

where v_{im} is the measured velocity of section i-i, e is the column number of the measuring point parallel to the short side of the rectangle, and f is the column number of the measuring point parallel to the long side of the rectangle.

The cross section of the tunnel was measured using a laser profiler before the determination of the location of measure points. Take section 4-4 as an example, its size and shape are shown in Figure 5 after the measurement by the laser profiler. An improved log-Tchebycheff method was then used because that the cross section was not a rectangle. This means a weight in line with the length of the measurement line was considered when calculating the air flow rate of the tunnel section. To achieve high precision, adjustments to the position of the measurement line of two adjacent wall edge regions had to be made. Specifically, if six measurement lines were used in the in situ test, then $X_{\mathrm{I}}/L = 0.075$ and $X_{\mathrm{N}}/L = 0.925$, and if seven were used, then $X_{\mathrm{I}}/L = 0.065$ and $X_{\mathrm{N}}/L = 0.935$ (ISO 5802: 2001,1DT). The position of the middle lines can be checked in Table 2.

The measuring point distribution based on the log-Tchebycheff method is shown in Figure 5. Measuring lines 1 to 6 are shown from left to right, and the specific values are listed in Table 2. The TF-3 ventilator comprehensive tester applied in this test is shown in Figure 6.

The volume flow rate of the entire air duct can be expressed as follows:

$$q_{4v} = \left[(v_1 l_1) + (v_2 l_2) \cdots (v_N l_N)\right] \frac{L}{N_{\mathrm{r}}} \tag{15}$$

where $q_{4\mathrm{v}}$ is the total volume flow of section 4-4, v_{N} is the arithmetic average velocity at the measuring point of the Nth measuring line, L_{N} is the length of the Nth measuring line, and N_{r} is the total number of measuring lines. L is the length of the baseline between the tunnel surfaces.

The axial fan air flow rate can be then calculated as follows:

$$q_{\mathrm{v}} = \frac{q_{\mathrm{m}}}{\rho_3} = \frac{\rho_4 q_{4\mathrm{v}}}{\rho_3} \tag{16}$$

where q_{v} is the axial fan flow rate.

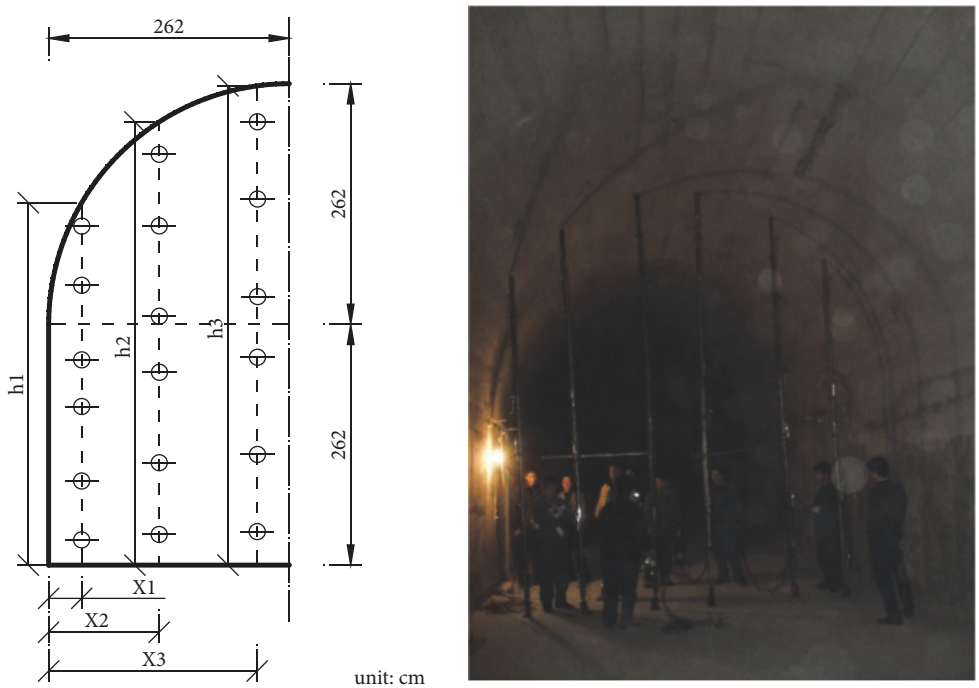

Figure 5: Test line and point distribution according to log-Tchebycheff method.

Figure 6: TF-3 ventilator comprehensive tester.

3.2.2. Fan Total Pressure. The total pressure of the axial fan can be expressed as follows:

$$p_t = p_3 - p_2 + \sum \Delta p \tag{17}$$

where p_t is the axial fan total pressure, p_i is the total pressure of section *i-i,* and Δp is the pressure loss caused by the fan collector and diffusion tube.

In (17),

$$p_i = p_{is} + \frac{\rho_i v_i^2}{2} \quad (i = 2, 3) \tag{18}$$

where p_{is} is the absolute static pressure of section *i-i* and can be calculated by (19) and v_i can be expressed by (20) and (21).

$$p_{is} = p_{isr} + p_a \quad (i = 2, 3) \tag{19}$$

$$v_2 = \frac{q_m/\rho_2}{S_2} \tag{20}$$

$$v_3 = \frac{q_v}{S_3} \tag{21}$$

In (20) and (21), S_2 and S_3 are the areas of sections 2-2 and 3-3, respectively. In (19), p_{isr} is the relative static pressure which can be determined by the U-shaped manometer:

As shown in Figure 7, four hydrostatic test holes were made in sections 2-2 and 3-3. These were connected to a single pressure transmission pipe, which was then connected to a U-shaped manometer. The result shown by the U-shaped manometer was the relative static pressure of the inlet and outlet of the fan.

The value of $\sum p$ can be expressed as follows:

$$\sum \Delta p = \left(\frac{\zeta_c \rho_2 v_{fi}^2}{2} + \frac{\zeta_d \rho_3 v_3^2}{2} \right) \tag{22}$$

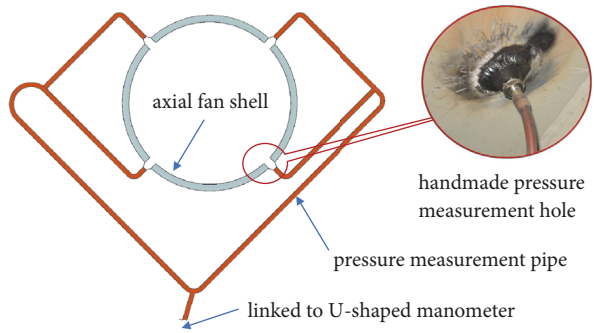

Figure 7: Homemade pressure test holes.

where ζ_c is the collector tapered loss coefficient, ζ_d is the diffusion tube expansion loss coefficient, and v_{fi} is the fan inlet velocity and can be calculated as follows:

$$v_{fi} = \frac{q_m}{\rho_2 \cdot S_{fi}} \tag{23}$$

where S_{fi} is the area of the fan inlet.

3.2.3. Total Pressure Efficiency. The fan axial power can be expressed as follows:

$$P_a = P_1 \times \eta_m \times \eta_c \tag{24}$$

where P_a is the fan axial power, η_m is the motor efficiency based on the Chinese code of Guidelines for the Design of Ventilation of Highway Tunnels (JTG/T D70/2-02-2014)[31], the range of η_m is 90%–95% (η_m = 93% is used in the following calculation), η_c is the mechanical transmission efficiency between the motor and fan (η_c = 100%), and P_1 is the motor input power that can be measured by the DJYC motor economy tester with the measurement precision of level 1. Because the motor power supply voltage of the fan was 6 kV, which was higher than the direct measurement limit of the tester. A voltage transformer (PT) and current transformer (CT) were used for the indirect measurement.

Based on the measured fan axial power and the fan output power, which could be calculated using the fan flow rate and fan pressure, the fan total pressure efficiency η_t can be expressed by

$$\eta_t = \frac{P_t}{P_a} = \frac{q_v p_t}{1000 P_a} \tag{25}$$

where P_t is the fan output total pressure power.

3.2.4. Fan Motor Capacity Safety Factor. The axial fan motor capacity safety factor can be calculated by using the following equation:

$$k_l = P_1 \cdot \frac{1000\eta_t\eta_m}{q_v p_{tf}} \cdot \frac{273 + t}{273 + 20} \cdot \frac{p_0}{p_a} \tag{26}$$

where k_l is the axial fan motor capacity safety factor.

3.2.5. Standard Conditions Convention. In order to compare the performance of different types of axial fans, the test data calculation had to be converted to the situation with the rated fan rotational velocity and standard air state (with an atmospheric pressure of 101325 Pa, an air temperature of 20°C, a relative humidity of 50%, and an air density of 1.2 kg/m^3) in accordance with the law of similarity.

The following equations can be applied to transfer the calculated parameters into the rated fan rotational velocity and standard air state:

$$\begin{aligned} q_{vf} &= k_n \cdot q_v \\ p_{tf} &= k_\rho \cdot k_n{}^2 \cdot p_t \\ p_{sf} &= k_\rho \cdot k_n{}^2 \cdot p_s \\ P_{af} &= k_\rho \cdot k_n{}^3 \cdot p_a \\ P_{tf} &= k_\rho \cdot k_n{}^3 \cdot p_t \\ P_{sf} &= k_\rho \cdot k_n{}^3 \cdot p_s \end{aligned} \tag{27}$$

where q_{vf} is the converted air flow rate, p_{tf} is the converted fan total pressure, p_{sf} is the converted fan static pressure, P_{af} is converted fan shaft power, P_{tf} is the converted fan output total pressure power, P_{sf} is the converted fan output static pressure power, k_ρ is the air density conversion factor, k_n is the rotational speed conversion factor, and k_ρ and k_n can be expressed as follows:

$$k_\rho = \frac{1.2}{\rho_i} \tag{28}$$

$$k_n = \frac{N_0}{N_i} \tag{29}$$

where N_0 is the rated speed of the axial fan and N_i is the measured speed of the axial fan.

4. General Steps for Tunnel Axial Fan Assessment

A general framework with six steps for a tunnel axial fan assessment is recommended in Figure 8. The first two steps

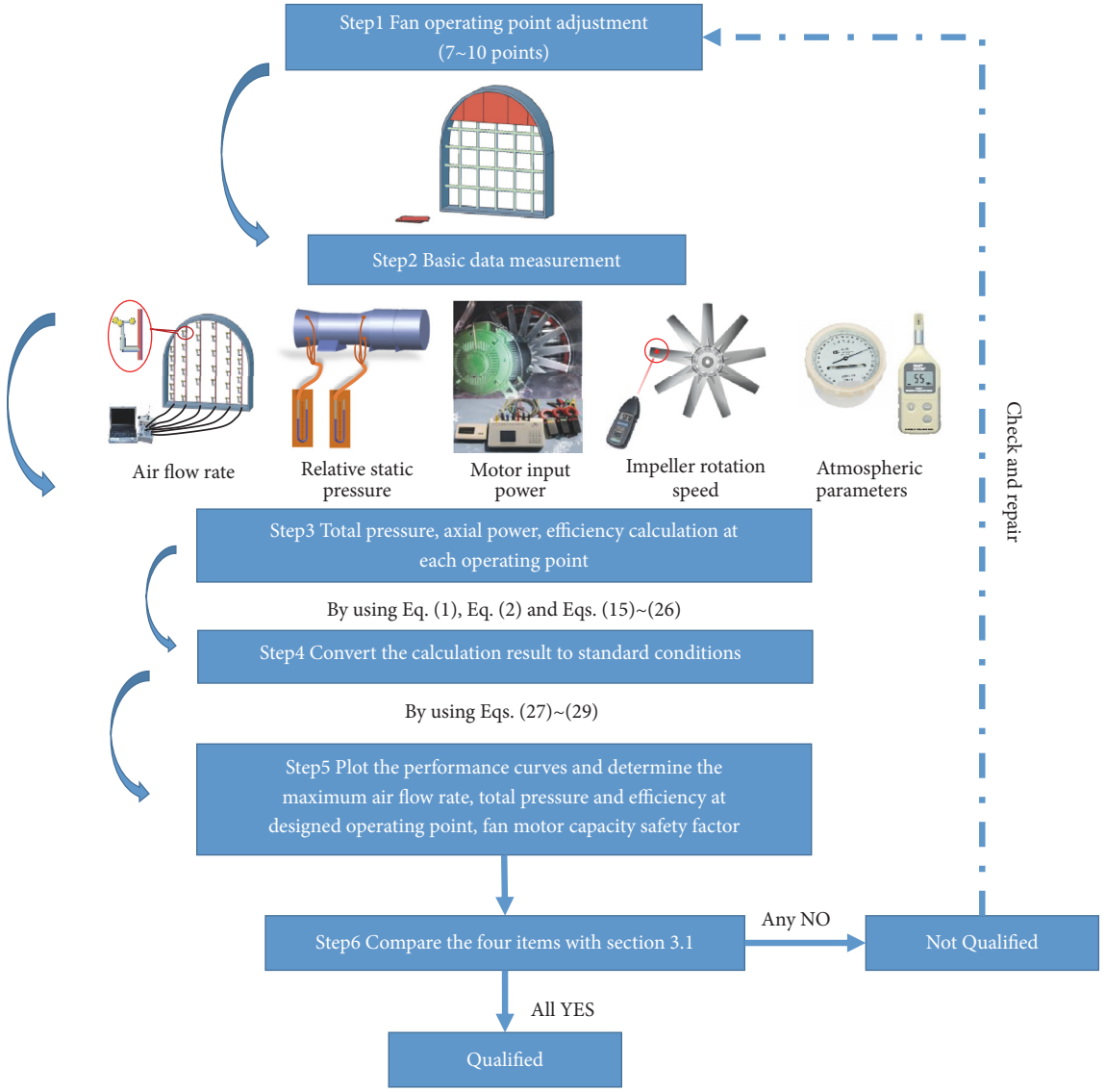

Figure 8: Axial fans assessment framework.

which are finished via the in situ test are followed by the calculation processes in steps 3, 4, and 5. Usually, seven to ten different operating points should be tested for the fitting of one performance curve. Then, a "YES" or "NO" can be obtained in step 6 by comparing the result from step 5 with the tunnel axial fan assessment criteria. If the fan is not eligible, more detailed electric tests should be carried out to check the problem of the fan and then have it fixed. Another performance in situ experiment should be carried out to test the fixed axial fan after the repairing.

5. Test Results and Discussion

5.1. Precision of the Log-Tchebycheff Method. The calculation of the fan flow rate by using log-Tchebycheff method is free from the multiple integral. Thus, the air flow rate can be easily determined. The air of the tunnel is treated as a fully developed turbulent flow when using the log-Tchebycheff method. However, the actual distribution of air flow in the tunnel differs from the ideal turbulent flow distribution. Another method to get a more accurate air flow rate is by fitting the flow field through the measured flow speed data and then calculates the volume enclosed by the 3D fitting surface and its projection plane. Biharmonic spline [35] interpolation method can be applied to solve this 3D interpolation problem.

The fitted flow field is shown in Figure 9. Taking the duct with direction as the x-axis and the duct height direction as the y-axis, the air flow rate is shown in the z-axis. The volume enclosed by the 3D fitting surface and its projection plane v can be expressed as follows:

$$v = \iint z(x, y)\,\mathrm{d}x\,\mathrm{d}y \tag{30}$$

Seven sets of experiments at the different operating point were carried out to get performance curves of the axial fan.

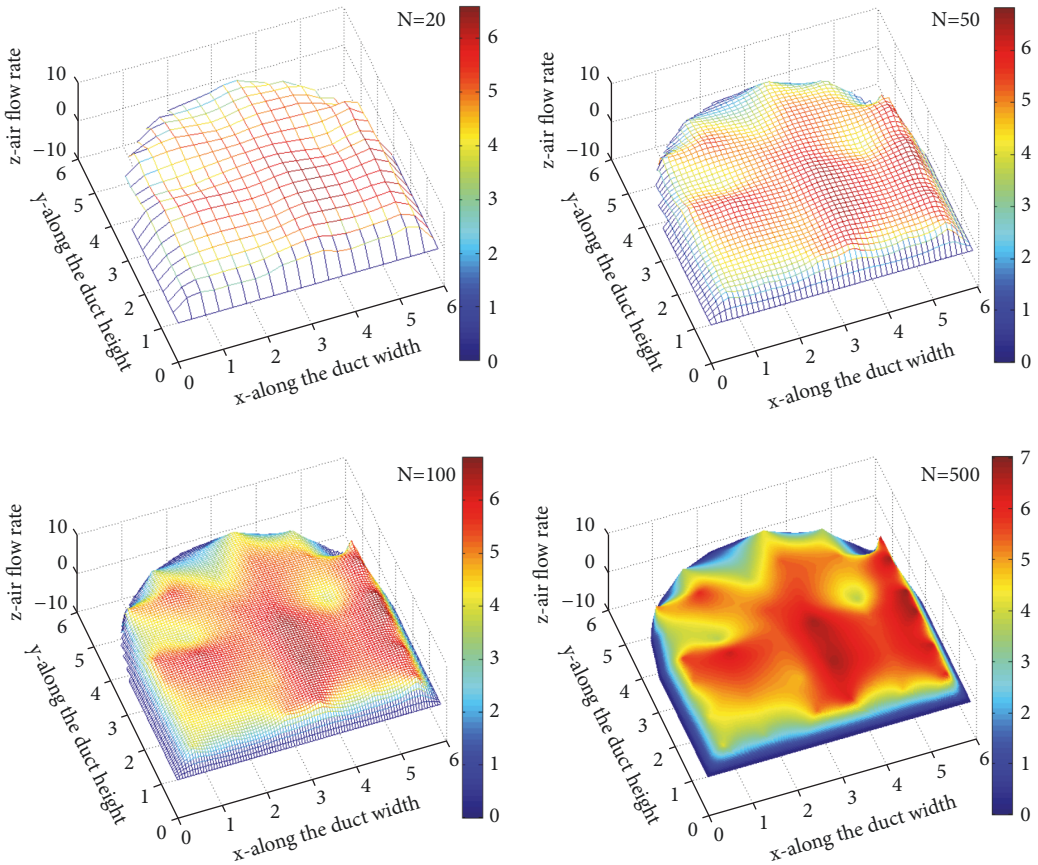

Figure 9: Smooth of the fitting surface influenced by the N.

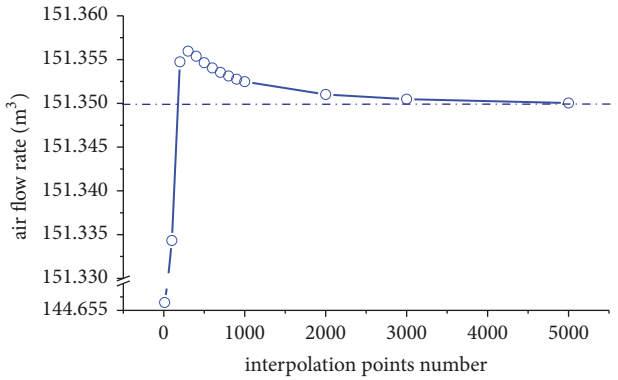

Figure 10: Air flow rate variation with N.

Take the first set of experiments as an example; the calculated air flow rate influenced by the interpolation points number is shown in Figure 9. It can be obtained from Figure 9 that the smooth of the fitting surface enhanced with the increase of the interpolation points number N from 20 to 500. It is obvious that the more interpolation points we take, the more precise of the integral result will be. More detailed from Figure 10, the air flow rate rises sharply before its peak at 300 and then declines smoothly. When N reaches to 2000, the calculation result tends to be stable. Thus, 2000 was chosen to be the number of interpolation points in the following calculations.

Comparison of the air flow rate results from the log-Tchebycheff method and MATLAB fitting are shown in Table 3, the difference between the two methods is about 4%. The log-Tchebycheff method showed high precision and great efficiency.

5.2. Fan Performance Assessment. According to the road tunnel axial fan assessment framework in Figure 8, curves are fitted in Figures 11–13 based on the in situ test data. Now we assess the axial fan along the assessment criteria in section 2.2.

Table 3: Air flow rate comparison.

Operating points		1	2	3	4	5	6	7
Air flow rate	Log-Tchebycheff method	157.65	151.12	149.79	141.96	138.89	130.97	119.57
	MATLAB fitting	151.35	145.23	143.74	136.19	134.40	125.58	114.80
Difference	(%)	3.99	3.90	4.04	4.07	3.23	4.12	3.99

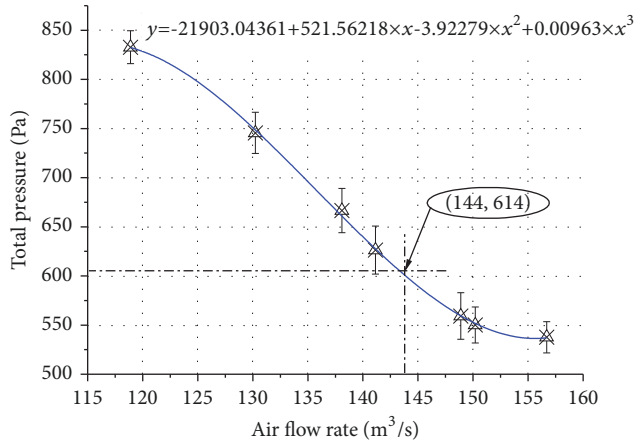

Figure 11: Air flow rate-total pressure curve.

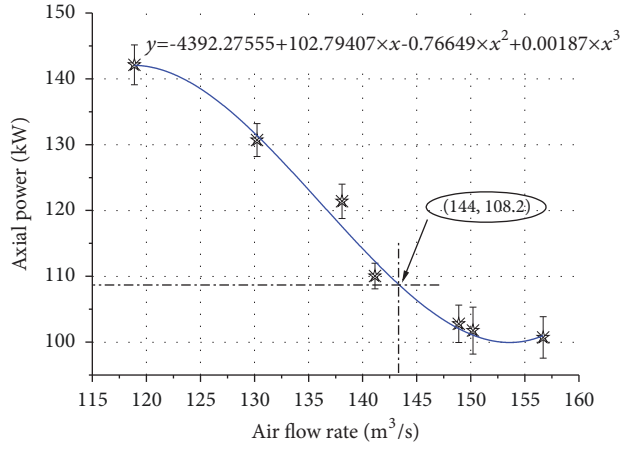

Figure 12: Air flow rate-axial power curve.

5.2.1. The Maximum Air Flow Rate. The maximum air flow rate of the tested fan is 157 m^3/s. It is bigger than the designed operating point of 144 m^3/s.

5.2.2. Difference between Tested Total Pressure and the Designed Total Pressure at Designed Operating Point. The tested total pressure at the designed operating point is 614 Pa (Figure 11). The difference is 2.5% when compared with the designed total pressure (630 Pa). It is smaller than the threshold of 5%.

5.2.3. Fan Motor Capacity Safety Factor. The in situ fan axial power at the designed operating point is 108.2 kW (Figure 12). The calculated fan motor capacity safety factor via (26) is 1.22 which satisfies the criteria.

5.2.4. Total Pressure Efficiency at the Designed Operating Point. It can be obtained from Figure 13 that the fan efficiency at the field environment is 78.6% which is more than 70%.

The assessment results of all the four items are "YES". Therefore, the tested axial fan of Qinling Zhongnan Mountain highway tunnel is qualified.

6. Conclusion

An in situ experiment to exam the axial fan performance of Qinling Zhongnan Mountain highway tunnels was carried out. Assessment criteria, test items, and methods for a qualified tunnel ventilation axial fan were recommended. A general framework for the road tunnel axial fan assessment was also provided. The log-Tchebycheff method to determine

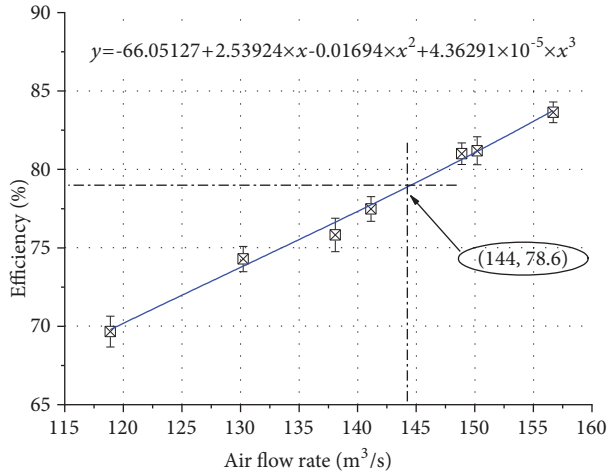

Figure 13: Air flow rate-efficiency curve.

the location of the air flow rate measurement points was proposed of which the precision was proven by comparing with the MATLAB fitting. Based on the investigations, the following conclusions are drawn:

(1) Axial fan assessment is an essential work for the safety and efficiency operating of the road tunnel ventilation system.

(2) The log-Tchebycheff method has qualified precision and good efficiency in measuring the air flow rate of a road tunnel.

(3) The 3D surface fitting of which the number of the interpolation point is recommended to be bigger than 2000 can be applied to obtain a more accurate result of the air flow rate.

Data Availability

The data used to support the findings of this study are included within the article.

Conflicts of Interest

The authors declare that they have no conflicts of interest.

Acknowledgments

The research work reported herein was made possible by the Ministry of Transport of the People's Republic of China (Grants no. 2013 318 802 400), Chang'an University (Grants no. 2008Z05), and Henan Provincial Department of Transportation (Grants no. 2017Z4). The financial support is highly appreciated.

References

[1] H. Bystroń, "The influence of dry mine air chemical composition on the safety state of the ventilation system of a deep mine using underground main fan," *Archives of Mining Sciences*, vol. 55, no. 3, pp. 377–387, 2010.

[2] Y. Dong and Z. Xinmin, "Research on ventilation quantity measuring method of mine main ventilator," *Coal Mine Engineering*, vol. 5, pp. 84–86, 2007.

[3] W. Dziurzynski, A. Krach, T. Palka et al., "Digital simulation of the gas-dynamic phenomena caused by bounce, experiment and validation," *Archives of Mining Sciences*, vol. 55, no. 3, pp. 403–424, 2010.

[4] F. Tang, Z. L. Cao, Q. Chen, N. Meng, Q. Wang, and C. G. Fan, "Effect of blockage-heat source distance on maximum temperature of buoyancy-induced smoke flow beneath ceiling in a longitudinal ventilated tunnel," *International Journal of Heat and Mass Transfer*, vol. 109, pp. 683–688, 2017.

[5] H. Cong, X. Wang, P. Zhu, T. Jiang, and X. Shi, "Experimental study of the influences of board size and position on smoke extraction efficiency by natural ventilation through a board-coupled shaft during tunnel fires," *Applied Thermal Engineering*, vol. 128, pp. 614–624, 2018.

[6] S. Takeuchi, T. Aoki, F. Tanaka, and K. A. M. Moinuddin, "Modeling for predicting the temperature distribution of smoke during a fire in an underground road tunnel with vertical shafts," *Fire Safety Journal*, vol. 91, pp. 312–319, 2017.

[7] F. Mei, F. Tang, X. Ling, and J. Yu, "Evolution characteristics of fire smoke layer thickness in a mechanical ventilation tunnel with multiple point extraction," *Applied Thermal Engineering*, vol. 111, pp. 248–256, 2017.

[8] M. Juraeva, K. Jin Ryu, S.-H. Jeong, and D. J. Song, "Influence of mechanical ventilation-shaft connecting location on subway tunnel ventilation performance," *Journal of Wind Engineering & Industrial Aerodynamics*, vol. 119, pp. 114–120, 2013.

[9] K. Wu, Q. Yang, C. Kang, X. Zhang, and Z. Huang, "Adaptive critic design based control of tunnel ventilation system with variable jet speed," *Journal of Signal Processing Systems*, vol. 86, no. 2-3, pp. 269–278, 2017.

[10] J.-H. Kim, J.-H. Kim, J.-Y. Yoon, Y.-S. Choi, and S.-H. Yang, "Application of multi-objective optimization techniques to improve the aerodynamic performance of a tunnel ventilation jet fan," *Proceedings of the Institution of Mechanical Engineers, Part C: Journal of Mechanical Engineering Science*, vol. 229, no. 1, pp. 91–105, 2015.

[11] C. Sarraf, H. Nouri, F. Ravelet, and F. Bakir, "Experimental study of blade thickness effects on the overall and local performances of a Controlled Vortex Designed axial-flow fan," *Experimental Thermal and Fluid Science*, vol. 35, no. 4, pp. 684–693, 2011.

[12] J.-H. Kim, J.-H. Kim, K.-Y. Kim, J.-Y. Yoon, S.-H. Yang, and Y.-S. Choi, "High-efficiency design of a tunnel ventilation jet fan through numerical optimization techniques," *Journal of Mechanical Science and Technology*, vol. 26, no. 6, pp. 1793–1800, 2012.

[13] C. M. K. Se, E. W. M. Lee, and A. C. K. Lai, "Impact of location of jet fan on airflow structure in tunnel fire," *Tunnelling and Underground Space Technology*, vol. 27, no. 1, pp. 30–40, 2012.

[14] F. Wang, M. Wang, and Q. Wang, "Numerical study of effects of deflected angles of jet fans on the normal ventilation in a curved tunnel," *Tunnelling and Underground Space Technology*, vol. 31, pp. 80–85, 2012.

[15] A. L. E. Sarmiento, W. de Oliveira, and R. G. R. Camacho, "Influence of the vortex design method in the performance characteristics of reversible axial rotors," *Journal of the Brazilian Society of Mechanical Sciences and Engineering*, vol. 39, no. 5, pp. 1575–1588, 2017.

[16] P. Prokop, P. Zapletal, and D. Fiuraskova, "Opeing of the sealed off working no. 28731 affected by spotaneoud combustion of coal," *Archives of Mining Sciences*, vol. 55, no. 3, pp. 537–546, 2010.

[17] C. Genyin and Z. Jinggang, "Measurement and analysis of main ventilator performance in xuzhuang mine," *China Safety Science Journal*, vol. 20, no. 2, pp. 104–109, 2010.

[18] J. Kruczkowski, "System for continuous measurement of volumetric rate of unsteady air flow in workings of deep mines," *Archives of Mining Sciences*, vol. 53, no. 4, pp. 533–544, 2008.

[19] P. Ligeza, E. Poleszczyk, and P. A. o. M. S. Skotniczny, "Method and the system of spatial measurement of velocity field of air flow in a mining heading," *Archives of Mining Sciences*, vol. 54, no. 3, pp. 419–440, 2009.

[20] Q. Wang, D. Shang, Z. Yang et al., "Design of Coal Mine Main Fan Performance Optimization," in *Proceedings of the 2009 Computational Intelligence and Industrial Applications, PACIIA '09*, vol. 2, 2009.

[21] W. Dziurzyński and J. Kruczkowski, "Variability of the volumetric air flow rate in a mine fan channel for various damper positions," *Archives of Mining Sciences*, vol. 56, no. 4, pp. 641–650, 2011.

[22] Y. Tong, X. Wang, J. Zhai, X. Niu, and L. Liu, "Theoretical predictions and field measurements for potential natural ventilation in urban vehicular tunnels with roof openings," *Building and Environment*, vol. 82, pp. 450–458, 2014.

[23] Y.-L. Qiu, N.-J. Li, and Y.-L. Xie, "Site test for ventilation resistance coefficient of shotcrete lining tunnel," *China Journal of Highway and Transport*, vol. 18, no. 1, pp. 81–84, 2005.

[24] Y. Wang, Y. Hu, M. Deng et al., "Complementary ventilation operational test in large longitudinal slope double-hole tunnel," *Journal of Traffic and Transportation Engineering*, vol. 14, no. 5, pp. 29–35, 2014.

[25] Y. Q. Wang, S. L. Zhang, F. Y. Xia et al., "Test on surface frictional resistant coefficient of ventilation shaft for tunnel," *Journal of Chang'an University*, 2015.

[26] Y. Fang, J. Fan, B. Kenneally, and M. Mooney, "Air flow behavior and gas dispersion in the recirculation ventilation system of a twin-tunnel construction," *Tunnelling and Underground Space Technology*, vol. 58, pp. 30–39, 2016.

[27] R. Ren, S. Xu, Z. Ren et al., "Numerical investigation of particle concentration distribution characteristics in twin-tunnel complementary ventilation system," *Mathematical Problems in Engineering*, vol. 2018, Article ID 1329187, 13 pages, 2018.

[28] P. Levoni, D. Angeli, E. Stalio, E. Agnani, G. S. Barozzi, and M. Cipollone, "Fluid-dynamic characterisation of the Mont Blanc tunnel by multi-point airflow measurements," *Tunnelling and Underground Space Technology*, vol. 48, pp. 110–122, 2015.

[29] Y.-R. Yang, C. He, and Y.-H. Zeng, "Research and field test about diffusion of exhaust gas from an extra long highway tunnel outlet," *Chinese Journal of Underground Space and Engineering*, vol. 2, p. 38, 2008.

[30] H.-T. Hu, G.-L. Ding, and K.-J. Wang, "Measurement and correlation of frictional two-phase pressure drop of R410A/POE oil mixture flow boiling in a 7 mm straight micro-fin tube," *Applied Thermal Engineering*, vol. 28, no. 11-12, pp. 1272–1283, 2008.

[31] Ministry of Communications of PRC, "Guidelines for Design of ventilation of Highway Tunnels," in *11 Fan selection and layout*, China Communications Press, China, 2014.

[32] N. Zhou and G. Liang, "The comparison of selection of different characteristic points with area velocity method," *Journal of China Institute of Metrology*, vol. 14, no. 2, pp. 104–108, 2003.

[33] Z. Xie, *Smart Instrument of Boiler Air Flow Measurement*, North China Electric Power University, 2004.

[34] Q. Li, N. Wang, and D. Yi, *Numerical Analysis*, Tsinghua University Press, Beijing, China, 2008.

[35] D. T. Sandwell, "Biharmonic spline interpolation of GEOS-3 and Seasat altimeter data," *Geophysical Research Letters*, vol. 14, no. 2, pp. 139–142, 1987.